Available online at www.sciencedirect.com
ScienceDirect
Polymer 47 (2006) 7535–7547
polymer
www.elsevier.com/locate/polymer

Gas permeation in poly(ether imide) nanocomposite membranes based on surface-treated silica. Part 2: With chemical coupling to matrix

S. Takahashi [a,b], D.R. Paul [a,b,*]

[a] Department of Chemical Engineering, The University of Texas at Austin, Austin, TX 78712-1062, USA
[b] Texas Materials Institute, The University of Texas at Austin, Austin, TX 78712-1062, USA

Received 14 July 2006; received in revised form 15 August 2006; accepted 16 August 2006
Available online 11 September 2006

Abstract

Nanocomposite membranes based on nano-sized SiO_2 particles with chemical coupling to the polymer matrix are described with special emphasis on gas permeation properties. In this paper, poly(ether imide) with reactive imide rings in the backbone was used as the matrix to which the SiO_2 particles were chemically bonded via an amine-containing silane coupling agent. Four types of nanocomposite membranes were prepared by solution casting and melt processing and characterized in terms of morphology and void volume formed due to adding SiO_2 particles. The relative gas permeability of the nanocomposite with chemical coupling to matrix was decreased by the presence of SiO_2 particles. Diffusion coefficients computed from time lag data also decreased with SiO_2 content. However, solubility coefficients computed by dividing the experimental permeability by the diffusivity obtained from the observed time lag increased with SiO_2 content contrary to simple composite theory. These permeation properties are discussed in terms of the void volume fraction estimated by density observations. In addition, TEM and SEM were used to explore the morphology of these nanocomposite membranes.

Keywords: Nanocomposites; Silica; Permeation

1. Introduction

There has been considerable interest in the addition of nano-sized particles to polymer matrices to alter properties [1–21]. Much of the research in this area has involved high aspect ratio nanoparticles like the aluminosilicate platelets that comprise natural minerals like montmorillonite, vermiculite, etc. [1–8]; however, in the membrane area there has been interest in using low aspect ratio nano-sized particles, like zeolites and silica, for altering the balance between permeability and selectivity for membrane separations [9–21]. A central question is whether the usual rules of composite theory apply or whether the presence of small, high surface area particles, where the interparticle distances are small, alter the local properties of the polymer matrix, e.g., by interfering with local segmental packing or alteration of the force field in which the segments move [16–20]. There are intriguing reports on beneficial separation characteristics of adding fumed silica particles to high free volume polymers like poly(4-methyl-2-pentyne) (PMP) or poly(2,2-bis(trifluoromethyl)-4,5-difluoro-1,3-dioxole-co-tetrafluoroethylene) [15–21]. These reports suggest that the nanoparticles in these cases do alter the properties of the matrix polymer.

In Part 1 of this series, we sought to determine whether addition of fumed silica to a conventional polymer with a more flexible backbone would lead to analogous changes that imply alteration of the matrix polymer; the commercial poly(ether imide) ULTEM® was chosen for this purpose [9]. It was found that formation of a homogeneous distribution of the fumed silica in ULTEM® is very challenging, and density and gas transport measurement strongly suggested that a small but very influential fraction of voids exist in these composites

* Corresponding author. Department of Chemical Engineering, The University of Texas at Austin, Austin, TX 78712-1062, USA. Tel.: +1 512 471 5392; fax: +1 512 471 0542.
E-mail address: drp@che.utexas.edu (D.R. Paul).

0032-3861/$ - see front matter © 2006 Elsevier Ltd. All rights reserved.
doi:10.1016/j.polymer.2006.08.036

regardless of the method of preparation. In that work, silica particles with various surface treatments on the surface, to make them more hydrophobic and to be better wetted by organic polymers, were used. However, the particles were not chemically bonded to the polymer matrix. In this paper, we use schemes to chemically bond the particles to the polymer matrix, using silane coupling agents, with the hope of eliminating any voids at the polymer–particle interface and, thus, to explore whether small, high surface area particles alter the properties of the ULTEM® matrix.

2. Experimental

2.1. Materials and chemical reaction strategy

This work used the same commercial poly(ether imide) ULTEM® 1000 from GE Plastics as in the first paper in this series [9]. Silicon dioxide, or SiO_2 (Silica), particles were obtained from Sigma–Aldrich which are claimed to be 10 nm in size and spherical in form with a BET surface area of 590–690 m^2/g and a density of 2.2 g/ml. The organofunctional silane, 3-aminopropyltriethoxysilane from Sigma–Aldrich, was used as a coupling agent. Silane coupling agents are frequently used in composites to bond glass particles or fibers to organic polymer matrices [22–25]. The silane units chemically react with the SiO_2 surface while the amine groups can react with the amide or imide units in the polymer backbone [22–25].

The chemical structure of this amine silane coupling agent and the expected reaction pathway are shown in Fig. 1. The amine silane coupling agent was added with stirring to deionized water to form a 2 wt% (2 g) mixture. At least 10 min was allowed for hydrolysis to form silanol. The solution was sonicated for a minute after 1.5 g of SiO_2 particles was added. The

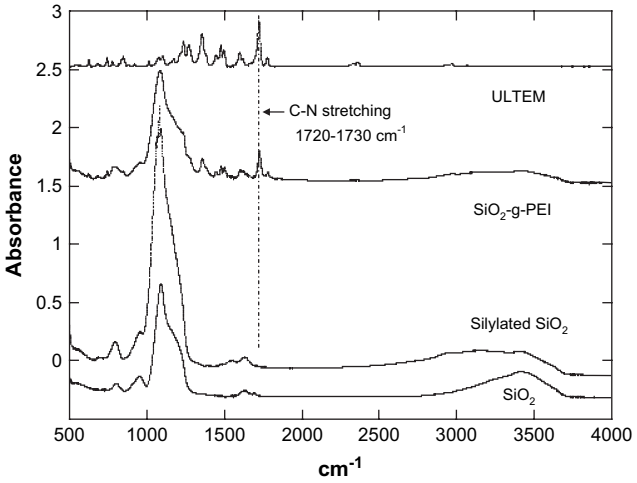

Fig. 2. FT-IR spectra of untreated and treated SiO_2 and ULTEM® polyetherimide.

SiO_2 particles were dried under vacuum above 120 °C prior to use because the surface generally contains absorbed water which might interfere with this process [26]. The resulting dispersion was stirred for a few days. The suspension was left quiescent to allow the silylated SiO_2 particles to settle which were subsequently removed from the mixture by decantation. The recovered silylated SiO_2 particles were rinsed by water a few times to remove excess amine silane coupling agent. Finally, the silylated SiO_2 particles were dried for a day under vacuum at 150 °C. The success of the above reaction was confirmed by detection of nitrogen atoms from the attached amine using XPS and by FT-IR spectroscopy (see Fig. 2).

After the above procedure, ULTEM® polymer chains were attached to the silylated SiO_2 particles via the reaction scheme

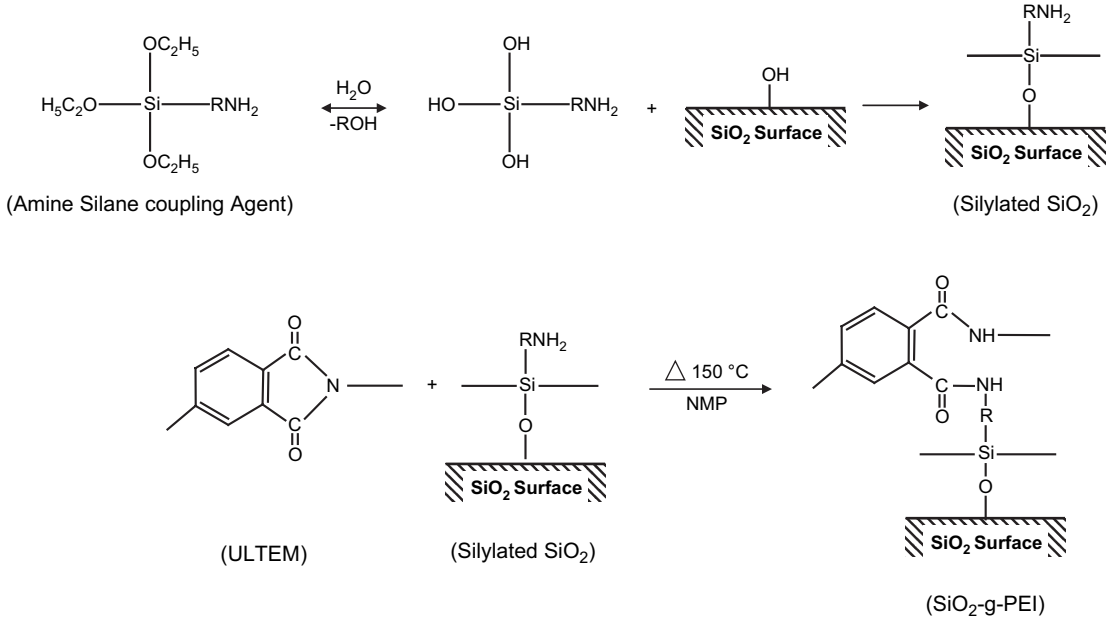

Fig. 1. Schematic of amine silane coupling agent reactions for bonding SiO_2 particles to polyetherimide.

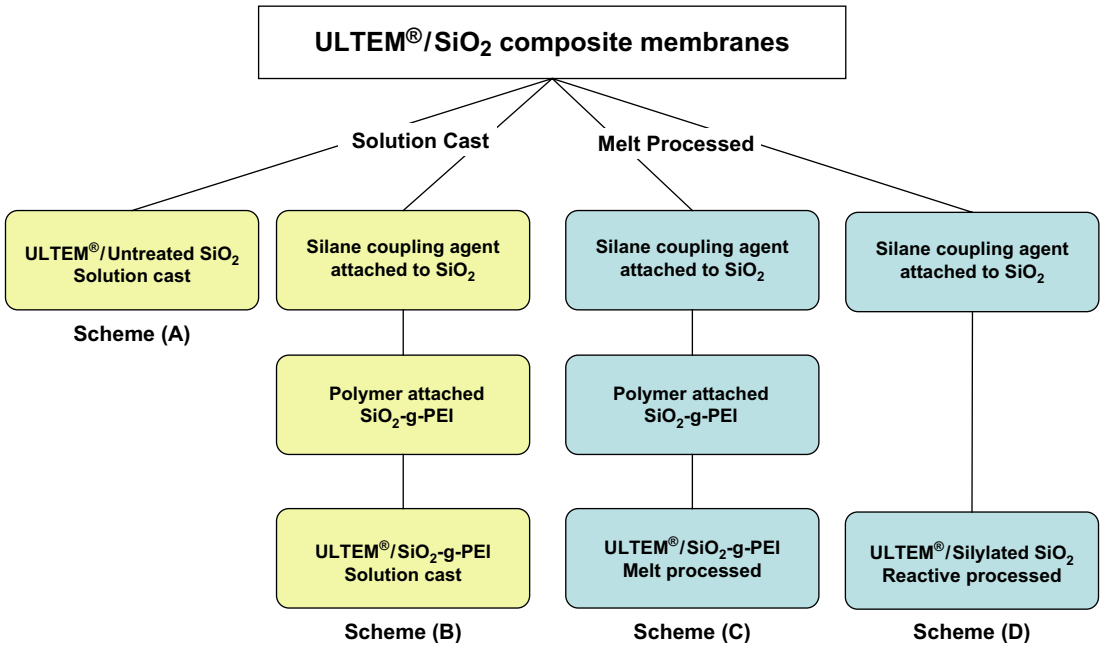

Fig. 3. Schemes used to prepare nanocomposite membranes for this study.

shown in Fig. 1. Polymer attachment to the silylated SiO_2 particles was carried out by adding the particles to a 10 wt% polymer solution in NMP solvent which was heated to 150 °C for 2 h. The mixture was cooled to room temperature where the polymer-treated SiO_2 particles, i.e., SiO_2-g-PEI, were removed from the mixture by decantation as previously described and then rinsed with methylene chloride to remove any unreacted polymer. SiO_2-g-PEI was dried under vacuum for 2 days at 160 °C and analyzed by FT-IR to confirm the success of the reaction (see Fig. 2).

In addition, the amount of coupling agent and polymer attached to the SiO_2 was determined by mass measurement before and after burning off the organics in a furnace at 900 °C for 45 min. According to this analysis the process described above led to the attachment of about 12 wt% silane coupling agent and about 18 wt% of polymer on the SiO_2.

Composite membranes were made by four different methods involving solution casting and melt processing as suggested in Fig. 3 for comparison. Thicknesses in the range of 30–50 μm were obtained by solution casting techniques; for reasons explained in the prior paper [9], the casting solvent was methylene chloride containing a small amount of chloroform. The ULTEM® polymer, solvent, and untreated SiO_2 (Scheme A in Fig. 3) or SiO_2-g-PEI (Scheme B in Fig. 3) were stirred for 10 min in a laboratory two-speed blender. The blended mixture was poured into flat Petri dishes and covered to allow slow solvent evaporation. Thickness of the films was determined by a micrometer. All of the nanocomposite membranes made by solution casting were annealed at 180 °C (just below the matrix polymer's T_g) for 2 h to remove residual solvent. Melt processed nanocomposite membranes made using a DSM micro-extruder followed by compression molding were prepared and compared with solution-cast films. The polymer and SiO_2-g-PEI were mixed at 100 rpm for 8 min, including sample loading time, in the micro-extruder, i.e., Scheme C in Fig. 3. In addition, reactively processed samples were also made by melt processing using the DSM micro-extruder. In this case, the polymer and silylated SiO_2, i.e., only the amine silane coupling agent was attached to the particle but no polymer, were mixed at 100 rpm for 8 min as for the former samples, i.e., Scheme D in Fig. 3. The screw and barrel temperature were set at 320 °C. In both cases, the melt strand was transferred to a compression molder preheated to 320 °C to press the melt into films about 200 μm thick. All samples were annealed overnight in a vacuum oven just below the glass transition temperature.

The amount of SiO_2 in each nanocomposite membrane was determined by burning the prepared membrane in a furnace at 900 °C for 45 min and measuring the residual SiO_2. All of samples used in this study are described in Table 1.

2.2. Measurements

The densities of neat ULTEM® and the various composite membranes were measured using a gradient column based on aqueous mixtures of calcium nitrate as described in the previous paper [9]. The theoretical bulk density of the nanocomposite was estimated from the composition and the density of the components assuming volume additivity. The excess volume was computed from the measured density of the composite and the theoretical density based on volume additivity; this may reflect actual voids, particularly around particles, a change in polymer free volume, or both. Errors associated with uncertainty in the effective particle density were described in the previous paper [9].

Table 1
Composition of nanocomposite samples used in this study

Preparation	Sample	SiO_2 type	SiO_2 content (wt%)	SiO_2 content (vol%)
Solution cast	ULTEM® (solution cast)		0.0	0.0
	Untreat-5	Untreated SiO_2	6.1	3.7
	Untreat-10		9.6	5.9
	Untreat-15		13.8	8.6
	Untreat-20		16.2	10.3
	g-PEI-5	SiO_2-g-PEI	4.0	2.4
	g-PEI-10		7.2	4.4
	g-PEI-15		11.5	7.1
	g-PEI-20		18.6	11.9
Melt processed	ULTEM® (melt processed)		0.0	0.0
	Reactive-1.3	Silylated SiO_2	1.3	0.8
	Reactive-3.9	(reactive	3.9	2.3
	Reactive-6.2	processed)	6.2	3.7
	Reactive-13.1		13.1	8.1
	g-PEI-21 (melt)	SiO_2-g-PEI	2.1	1.2
	g-PEI-4.4 (melt)		4.4	2.6
	g-PEI-8.8 (melt)		8.8	5.3

A JASCO Fourier transform infrared spectrometer FT/IR-4100 was utilized to characterize changes in the SiO_2 particle surface and follow the attachment of polymer and amine silane coupling agent in the range of 500–4000 cm^{-1}.

The glass transition temperature (T_g) of nanocomposite membranes was determined during heating in a Perkin–Elmer DSC-7 under a N_2 atmosphere. Samples sealed in an aluminum pan were heated from 50 °C to 300 °C at a scanning rate of 20 K/min two times. The T_g was calculated from the onset of the transition in the second scan.

Gas permeation through the nanocomposite assemblies was measured at 35 °C for He, O_2, N_2, CH_4 and CO_2 at an upstream pressure of about 28 psig (3 atm) using a constant volume/variable pressure type permeation cell used in this laboratory and described in detail elsewhere [27–28]. The traditional equations regarding the permeation and separation factor, α, were described in the previous paper [9].

Gas sorption isotherm measurements were carried out using a pressure decay method as a function of temperature in a dual volume apparatus described previously [29]. The effect of non-ideal gas behavior was accounted for by using compressibility factors [30].

Thin sections for transmission electron microscopy (TEM) ranging from 20 to 30 nm in thickness were cut with a diamond knife at a temperature of −40 °C using a Reichert-Jung Ultracut E microtome. In this process, the nanocomposite membranes were supported by epoxy resin to facilitate cutting. The sections were collected on 300 mesh square copper grids and subsequently dried with filter paper. The sections were examined by TEM using a JEOL 2010F TEM at an accelerating voltage of 120 kV.

A Hitachi S-4500 field emission scanning electron microscope (SEM), operated at a voltage of 15 kV, was used to view cross-sections formed by cleaving the nanocomposite with tweezers after immersion in liquid nitrogen and subsequently coated with gold.

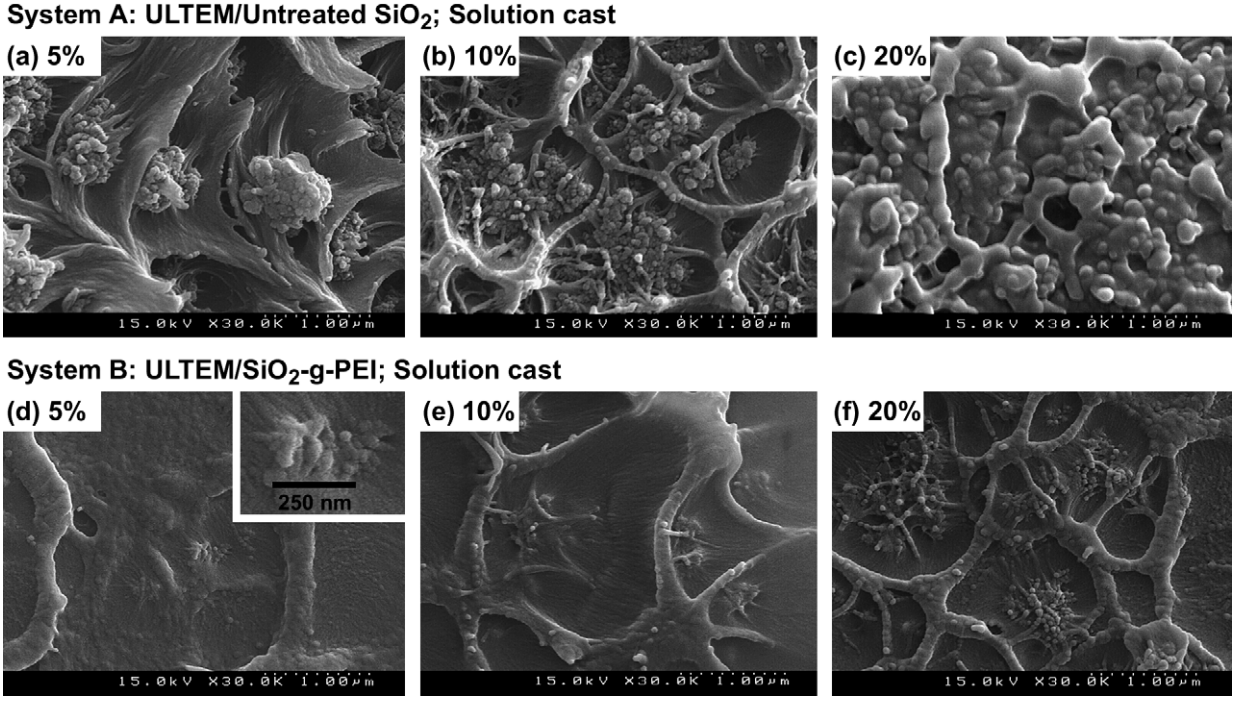

Fig. 4. SEM images of cryofractured cross-sections of ULTEM®/untreated SiO_2 composites, (a) 5 wt%, (b) 10 wt%, (c) 20 wt%, and of ULTEM®/SiO_2-g-PEI composites, (d) 5 wt%, (e) 10 wt%, (f) 20 wt%, prepared by solution casting.

3. Results and discussion

3.1. Chemical reaction

To confirm the attachment of the amine silane coupling agent to the surface of SiO_2 particles, both XPS and FT-IR measurements were made. The IR absorption by the amine group on the coupling agent, i.e., $-NH_2$; 3300–3500 cm^{-1}, may be overlapped with that of hydroxyl groups on the surface of the SiO_2 particles in the region of 3200–3570 cm^{-1} (see Fig. 2) so the spectra obtained are not completely conclusive. However, the XPS analysis revealed that the silylated SiO_2 particles contained 4.83% nitrogen. Burning off the organic components in a furnace indicated that the silylated SiO_2 particles contained 12 wt% amine silane coupling agent on the surface (see Section 2). Taken together, these tests provide strong evidence of the success of attachment of amine silane coupling agent to the SiO_2 particles.

SiO_2-g-PEI has the characteristic CN stretching absorption peaks of poly(ether imide) at 1720 and 1780 cm^{-1} and others along with the characteristic spectrum of native and silylated SiO_2. Also, the loss of organics during burn off in the furnace indicated that the SiO_2-g-PEI contains about 18 wt% poly(ether imide) coupled to the surface (see Section 2).

3.2. Electron microscopy observation

Figs. 4 and 5 show SEM images of fractured surfaces of composite membranes made by solution casting and melt processing, respectively. For the composite membrane made by solution casting, the effect of polymer grafting via the coupling agent, see Fig. 4(d)–(f), was clarified by comparing with SEM images of composites including untreated SiO_2, see Fig. 4(a)–(c). It is clearly recognized from Fig. 4(a) and (b) that composite membranes made from untreated SiO_2 form particle agglomerates in the polymer matrix even at very low contents of filler. The composite membranes based on SiO_2-g-PEI also show particle agglomeration in the matrix but the particles seem to be well covered by the polymer. Composite membranes made by melt processing, see Fig. 5, also show agglomerated particles covered by polymer matrix on the fracture surface as well as composite membranes based on SiO_2-g-PEI.

TEM images provide additional understanding of the morphology achieved. Solution-cast membranes containing untreated SiO_2 and SiO_2-g-PEI in varying amounts are shown in Fig. 6. Samples containing 10 and 20 wt% of SiO_2 from SiO_2-g-PEI and untreated SiO_2 prepared by solution casting are compared. In all cases, the samples contain agglomerated SiO_2 particles, sizes >200 nm, which become larger with increased SiO_2 content. However, at high SiO_2 contents, the agglomerates formed from SiO_2-g-PEI appear to be smaller than those from untreated SiO_2. Images for melt processed composite membranes are shown in Fig. 7; in all cases, there is better SiO_2 particle dispersion than seen in the solution-cast

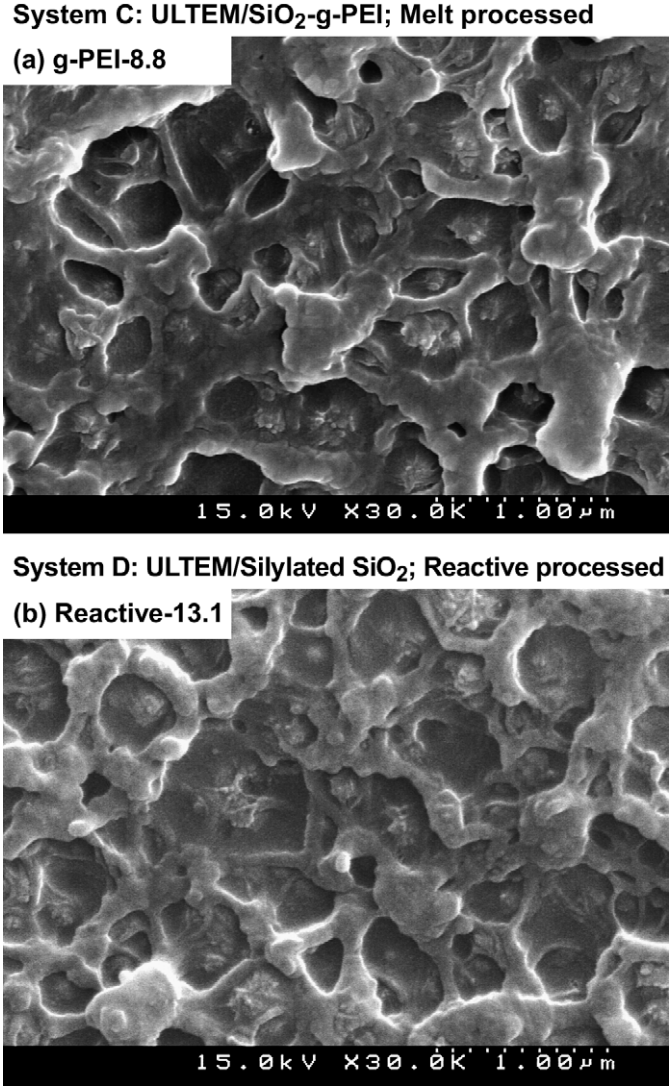

Fig. 5. SEM images of cryofractured cross-sections of (a) ULTEM®/SiO_2-g-PEI 8.8 wt% and (b) ULTEM®/silylated SiO_2 13.1 wt%.

samples. The high shear mixing by melt processing along with chemical coupling to the polymer matrix results in better dispersion of the filler. Nanocomposite membranes formed from SiO_2 particles where the PEI was attached in a prior step showed relatively larger agglomerates of SiO_2 particles, see Fig. 7(b). Samples formed by reactive processing using sylilated SiO_2 particles (without previous reaction with PEI) showed the best filler dispersion. In the routes involving silica particles with grafted ULTEM®, i.e., SiO_2-g-PEI, it is possible that particle agglomerates were formed in the reaction step and could not be separated into individual particles thereafter. On the other hand, during reactive melt processing, the chemical reaction occurs only during the high shear, dispersive mixing step which may discourage particle agglomeration.

3.3. Density and thermal characterization

Fig. 8 shows the glass transition temperature, T_g, of the pure ULTEM® and various nanocomposites studied here as

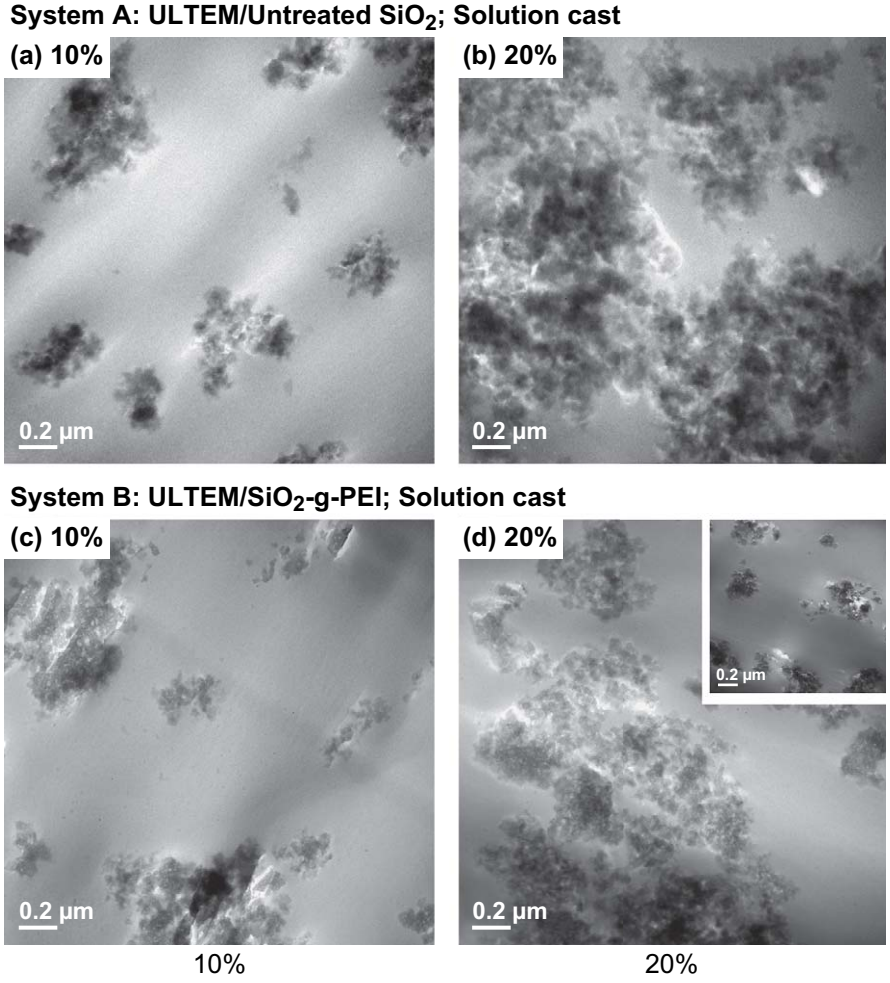

Fig. 6. A series of TEM images of nanocomposite membranes prepared by solution casting. ULTEM®/untreated SiO_2: (a) 10 wt%, (b) 20 wt%, and ULTEM®/SiO_2-g-PEI: (c) 10 wt%, (d) 20 wt%.

a function of SiO_2 content. The nanocomposite membranes made by solution casting tend to have a slightly higher T_g than pure ULTEM® while those made by melt processing tend to be even higher. The same tendency was shown in the previous paper [9]. The extensive drying protocol would seem to rule out residual solvent as a significant source for reducing T_g. However, all of nanocomposite membranes made by solution casting have effectively been annealed just below T_g prior to use since this was the protocol for solvent removal.

Density measurements provide a convenient way to evaluate the extent of voids in the internal structure of composites. TEM and SEM are useful for visualizing the composite morphology but do not readily reveal some of the structural defects that affect gas permeation properties. Theoretically, if we know the composition and densities of pure matrix and filler, the density of the composite should be predictable from volume additivity. However, as shown in the previous paper [9], in many cases voids or defects are formed and the actual density is consistently lower than the theoretical value because the filler forms agglomerates and wetting at the interface between matrix and filler is poor. Overcoming this is a key issue of this paper.

The measured densities of the various nanocomposite membranes described above were lower than that of the theoretical density calculated by volume additivity. The density of solution-cast nanocomposites showed prominent deviations from additivity even at low SiO_2 content. This deviation was expressed as a percent void volume as described previously [9] and is shown in Fig. 9. The calculated void volume percent increases with increasing fumed silica loading in all cases. The void content is strongly affected by the processing method. Interestingly, for nanocomposites made by solution casting, the void volume increases rapidly with SiO_2 particle content and then levels off. On the other hand, the void volume of nanocomposite membranes made by melt processing increased gradually with increased SiO_2 content. The chemical coupling to the matrix reduced the void volume but apparently did not completely eliminate void formation. It is important to recognize that the very large volume change associated with evaporation of the solvent apparently is a prime mechanism for void formation in such composites. Melt processing should

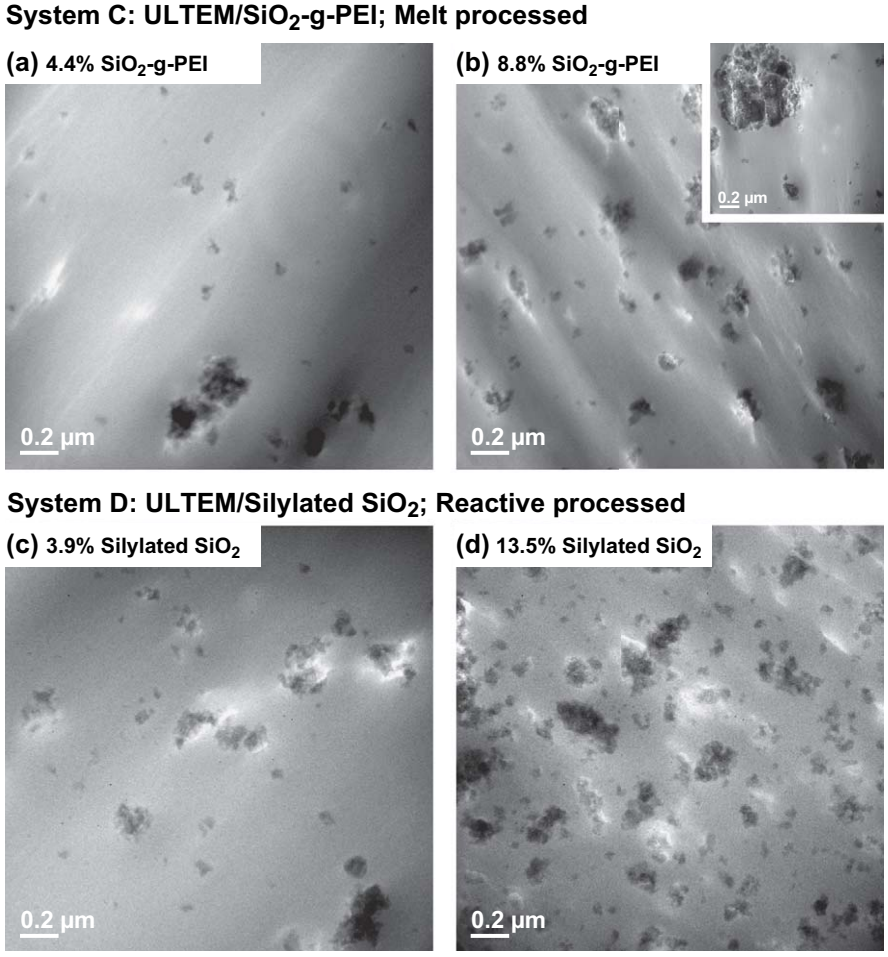

Fig. 7. A series of TEM images of nanocomposite membranes prepared by melt processing. ULTEM®/SiO_2-g-PEI: (a) 4.4 wt%, (b) 8.8 wt%, and ULTEM®/silylated SiO_2: (c) 3.9 wt%, (d) 13.5 wt%.

remove this mechanism of void formation; however, thermal shrinkage, entrapped air, etc., represent other causes of void formation in this process. In addition, ULTEM®/SiO_2-g-PEI composite membranes made by solution casting had larger void volume than that of ULTEM®/untreated SiO_2. This is an intriguing result and possible explanations will be described later. Among the melt processed nanocomposite membranes, the reactively processed samples had lower void

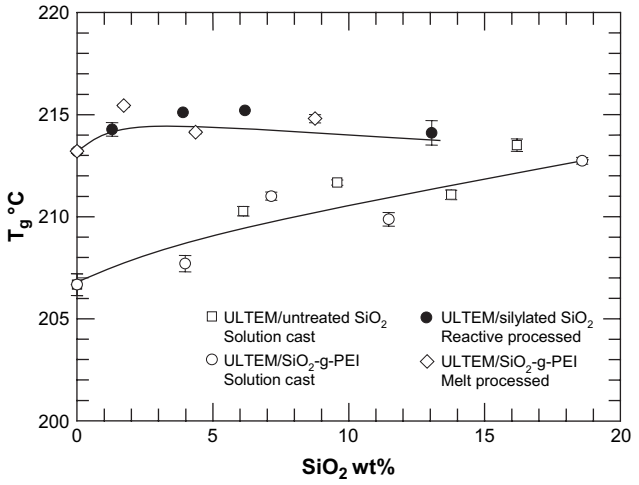

Fig. 8. Variation in glass transition temperature, T_g, of nanocomposites based on SiO_2 made by solution casting and melt processing as a function of SiO_2 content.

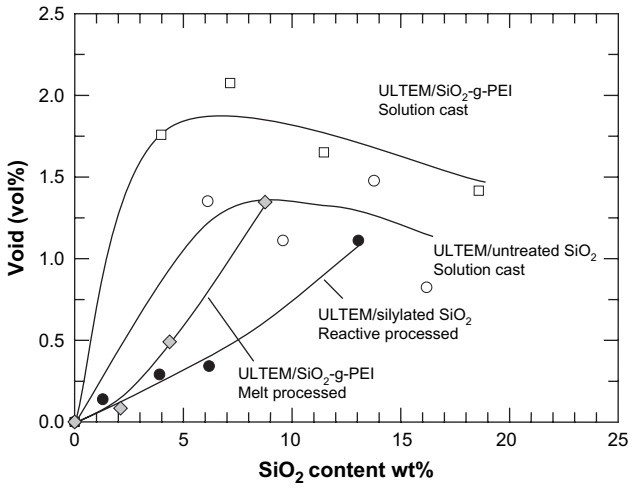

Fig. 9. Void volume fraction of nanocomposites made by solution casting and melt processing as a function of SiO_2 content. Density of SiO_2 is assumed to be 2.2 g/cm^3.

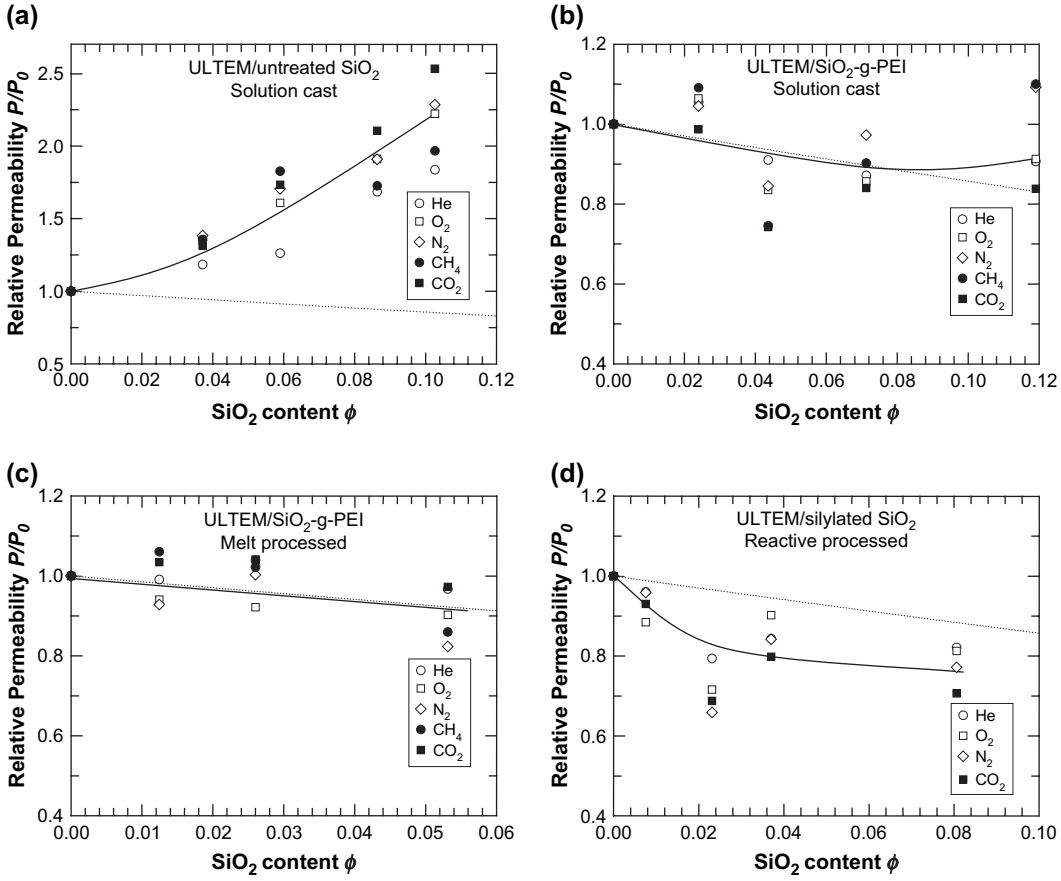

Fig. 10. Relative permeability of various gases in nanocomposites made by solution casting, (a) ULTEM®/untreated SiO_2, (b) ULTEM®/SiO_2-g-PEI, and by melt processing, (c) ULTEM®/SiO_2-g-PEI, (d) ULTEM®/sylilated SiO_2 (reactive processing), as a function of SiO_2 content. Measurements were carried out at 35 °C and 3 atm.

volume. This result is consistent with the better dispersion of SiO_2 particles seen in the TEM pictures (see Fig. 7(c) and (d)).

The nanocomposite membranes based on surface-treated fumed silica, but without chemical reaction between the matrix and filler, had 3% void volume at most and as little as 0.2%; whereas, the nanocomposite membranes including SiO_2 with chemical coupling to the matrix had 2% void volume at most. Thus, the chemical coupling strategies seemed to reduce, but did not completely eliminate, void formation.

If the voids form channels that extend from one face of the membrane to the other, there can be a profound effect on gas permeation behavior like that shown in the prior paper [9]. Permeation behavior for the current composites is described in Section 3.4.

3.4. Steady-state permeation properties

Fig. 10 shows the permeability of several gases for the various composites made by solution casting and melt processing as a function of the volume fraction of fumed silica, ϕ. The prediction from the Maxwell theory for an impermeable spherical filler is shown as the dotted line for reference [31]. The permeability of the composite for a given gas is expressed relative to the permeability of that gas in pure ULTEM®, P_0. Values of P_0 are given in Part 1 of this series [9]. For composites made by relative processing, the films were too thick, ~200 μm, to measure CH_4 permeability. According to the theory described in the previous paper [9], the relative permeability for an ideal composite membrane should be the same for all penetrant gases if the particles do not affect the local properties of the matrix polymer. Voids around particles will increase the permeability of each gas but the relative permeability should be the same regardless of gas type assuming that there is no effect of the particle on the local matrix properties. The relative permeability of the various gases for the solution-cast nanocomposites formed from the untreated SiO_2 increases as the content of particles increase (see Fig. 10(a) and (b)) which is qualitatively similar to the observations for the various composites without chemical coupling described in the prior paper [9]. However, when the SiO_2 particles are chemically attached to the ULTEM matrix, the relative permeability tends to decrease with particle loading but the extent of decrease depends somewhat on the method of preparation, see Fig. 10. The magnitude of the decrease is comparable to that predicted by Maxwell's theory, but the extent of decrease may be more or less than this prediction, as seen in Fig. 10, depending on processing

details. In some cases, the relative permeability seems to show some trend with gas type but there are counter examples which make it difficult to discuss any specific trend. Broadly speaking, it appears that the experimental relative permeability versus particle content relation is essentially the same for all gases. We will examine this point in other ways later.

As noted earlier, these composites have somewhat lower densities than additive which may be interpreted as evidence for voids (see Fig. 9). However, it is difficult to see a clear trend between the permeability results and the density observations. Actually, a detailed understanding of the permeation results would require consideration of the state of agglomeration of the particles since the effective particle from the point of view of gas permeation is not the ultimate SiO_2 particles, see schematic illustrations in Fig. 11. The effective volume fraction of the agglomerates varies depending on how much matrix polymer is occluded in them. At some level, voids detected by density measurements may be inside the agglomerated particles and, therefore, contribute little to the transport behavior.

3.5. Time lag results

Time lag, θ, measurements were made for nanocomposite membranes as described above for all of the gases except helium, which was too short to be measured, and methane in some cases when the samples were too thick. Apparent diffusion coefficients were calculated from $D_a = l^2/6\theta$ where l is the film thickness.

Fig. 12 shows the apparent diffusivity coefficients normalized by the diffusion coefficient for that gas in ULTEM®, i.e., D_0, which were also determined from time lag data, as a function of SiO_2 content. Theoretically, the relative diffusion coefficient, like the relative permeability, should be independent of gas type and decrease with the SiO_2 content. However, the relative diffusivity of nanocomposite membranes without chemical coupling to the matrix, i.e., nanocomposites containing untreated SiO_2, increases with the addition of silica particles. This may indicate that voids exist in these nanocomposites. Nanocomposite membranes with chemical coupling to polymer matrix show a decrease in the relative diffusivity with an increase of SiO_2 volume fraction (see Fig. 12(b)–(d)). The reactive processed nanocomposite membranes (Fig. 12(d)) showed a greater reduction than any others. It is more likely due to a limited void volume fraction and the condition of filler dispersion. Also, ULTEM/SiO_2-g-PEI nanocomposite membranes (Fig. 12(b)) made by solution casting had larger agglomerated filler particles but showed lower relative diffusivity than the theoretical dotted line. We believe voids were formed just around particles (like Fig. 11(b)) in spite of filler agglomerates and penetrant gases mainly permeate the polymer matrix with a somewhat tortuous path.

Fig. 13 shows relative solubility for several gases in various nanocomposites; this was calculated by dividing the relative permeability by the relative diffusivity as suggested by simple

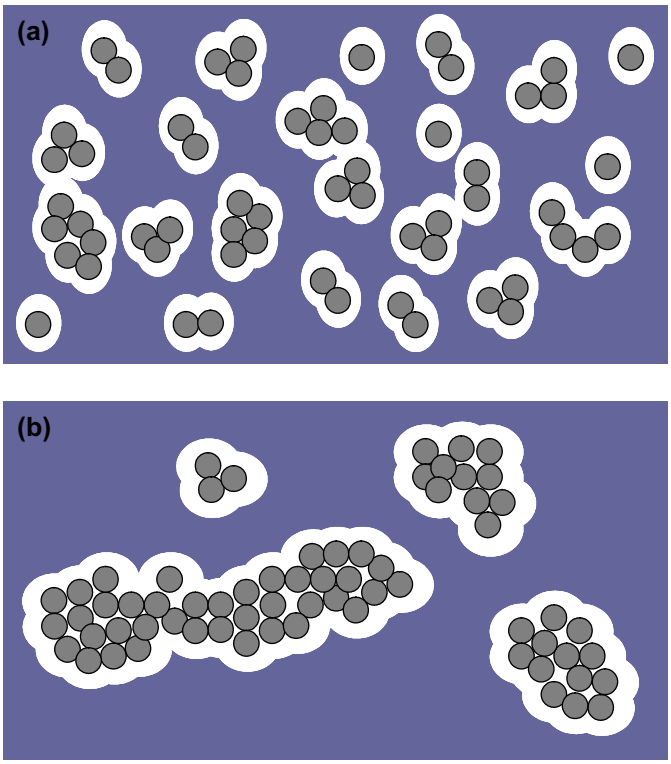

Fig. 11. Schematic illustrations of possible morphologies of composite membranes containing spherical filler particles that are partially fused together. (a) Dispersed filler and voids, (b) agglomerated filler and voids.

composite theory for non-sorbing particles. This theory predicts that the relative solubility, S_a/S_0, should be $1-\phi$, i.e., a decrease with increase in SiO_2 content. However, the relative solubility of nanocomposite containing untreated SiO_2 increases with the addition of silica particles (see Fig. 13(a)). Nanocomposite membranes with chemical coupling to polymer matrix have also shown an increase in relative solubility with an increase of SiO_2 content contrary to the theory. These results may reflect the presence of voids in addition to sorption in the matrix polymer plus possibly some contribution of adsorption by the filler or at the filler–matrix interface [32–33]. In nanocomposite membranes containing untreated SiO_2, CO_2 solubility characteristically increased with SiO_2 loading.

In addition, independent gas sorption experiments were made for CO_2 in pure ULTEM® and several nanocomposite membranes containing higher amounts of SiO_2 for better understanding; the results are shown in Fig. 14. The neat ULTEM® and other nanocomposite membranes show dual mode type sorption behavior as expected for a glassy polymer [34]. Nanocomposite samples, except for the composite containing untreated SiO_2, showed a slightly greater or almost the same sorption isotherm as the matrix polymer. This sorption behavior may be due to adsorption on the filler or at the filler–polymer interface. Nanocomposite membranes containing untreated SiO_2 showed a distinctly greater CO_2 sorption. As described in the previous paper [9], the extent of sorption increase relative to the matrix

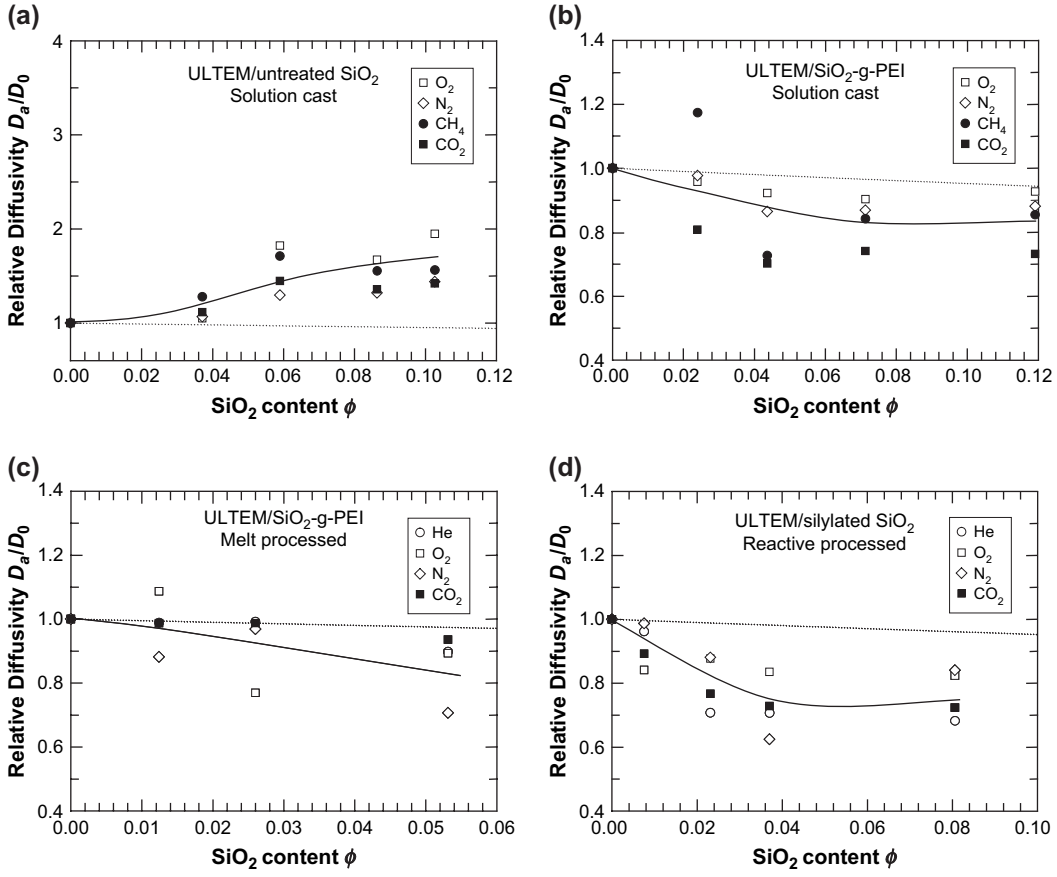

Fig. 12. Relative diffusivity of various gases in nanocomposites made by solution casting, (a) ULTEM®/untreated SiO_2 and (b) ULTEM®/SiO_2-g-PEI, as a function of SiO_2 content, and by melt processing, (c) ULTEM®/SiO_2-g-PEI, (d) ULTEM®/sylilated SiO_2 (reactive processing). Diffusivity was calculated from time lag measurements. The dotted line is Maxwell's prediction.

depends on the surface treatment. This may reflect the effect of sorption on the untreated SiO_2 filler with hydroxyl groups plus some effect of the filler–polymer interface.

3.6. Pure gas selectivity

Pure gas selectivities for O_2/N_2 and He/CO_2 can be calculated from the steady state permeability coefficients and are shown in Fig. 15. We can expect these ratios to be independent of filler content and reflect the characteristics of the pure matrix in the absence of voids and any effect of the filler on the matrix. A similar result would also be expected if voids are present so long as the morphology is like that suggested in Fig. 11(a) or (b). $P(O_2)/P(N_2)$ selectivity of nanocomposite membranes was almost maintained with an increase of SiO_2 content. The permeation of the smallest possible penetrant, He, ought to be least sensitive to any particle-induced changes in the local matrix properties. It is well known that changes in polymer chain packing and dynamics have a much greater effect on the transport of large penetrants than small ones like helium [35]. Thus, if the presence of the nanoparticles alters the packing, dynamics, or conformation of the polymer chain near its surface, then the ratio of the transport properties of larger penetrants like CO_2 to helium will be sensitive to this. Fig. 15 compares the effect of penetrant size on the permeability of the penetrant in the composite versus that dependence in the pure matrix. Nanocomposites containing SiO_2 not chemically coupled to the matrix show a gradual decrease in selectivity with increased SiO_2 content [9]. However, nanocomposite membranes with chemical coupling to the polymer matrix generally maintain the selectivity with an increase of SiO_2 volume fraction. This suggests that the presence of these particles has only a minor, if any, effect on permeation properties of the matrix. Note that the method of preparation has a noticeable effect on selectivity in most cases.

4. Conclusions

The objective of this work was to eliminate the voids formed by adding SiO_2 particles to a glassy polymer matrix with the hope of minimizing their obscuring effect on permeation properties of the composite. The approach used was chemical coupling of the SiO_2 particles to the polymer matrix via a silane coupling agent using various solution casting and melt processing methods. SEM and TEM techniques were used to show the state of filler particle dispersion for the

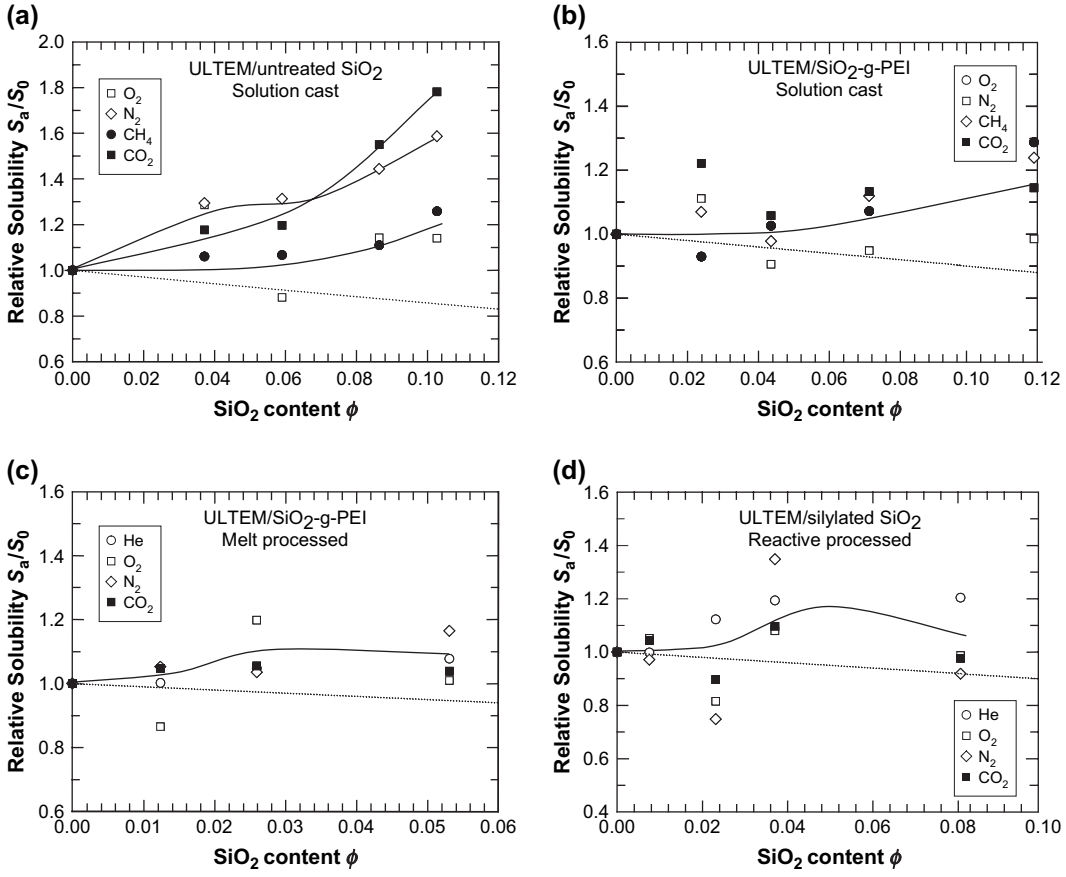

Fig. 13. Relative solubility of various gases in nanocomposites made by solution casting, (a) ULTEM®/untreated SiO_2, (b) ULTEM®/SiO_2-g-PEI, and by melt processing, (c) ULTEM®/SiO_2-g-PEI, (d) ULTEM®/sylilated SiO_2 (reactive processed), as a function of SiO_2 content. Solubility coefficients were calculated by dividing the permeability by diffusivity. The dotted line is the theoretical prediction.

different preparation methods. Nanocomposite membranes made by solution casting show larger agglomerated filler particles and greater void volume fraction than melt processed samples. In addition, reactive processed samples used sylilated SiO_2 had lower void volume. The chemical coupling strategy reduced the void volume but did not entirely eliminate void formation. The relative gas permeability and diffusivity of the nanocomposite with chemical coupling to matrix was decreased by the presence of SiO_2 particles. However, solubility coefficients computed by dividing the experimental permeability by the diffusivity from time lag measurements increased with SiO_2 content contrary to simple composite theory. These results are consistent with voids around and within agglomerated SiO_2 particles. For some preparation methods, the selectivity of gas transport was decreased by addition of particles, in spite of the chemical coupling to polymer matrix, presumably due to void formation. Other preparation methods with chemical coupling to the polymer matrix maintained selectivity equivalent to the matrix polymer as the SiO_2 volume fraction increased. For certain processing procedures, this chemical coupling strategy did reduce the void content in SiO_2/polyetherimide composites; however, even the best methods did not entirely eliminate all voids. The nano-sized SiO_2 particles formed agglomerates and were not individually dispersed. The results do not suggest any significant effect of the particles on the local properties of matrix particles; however, better dispersion will be needed to fully test this possibility.

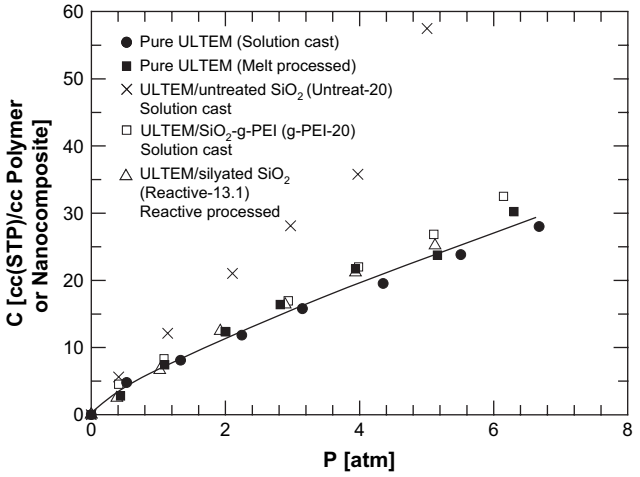

Fig. 14. Representative experimental CO_2 sorption isotherms for (a) pure ULTEM® prepared by solution casting, (b) g-PEI-20 made by solution casting and (c) reactive-13.1 made by reactive melt processing.

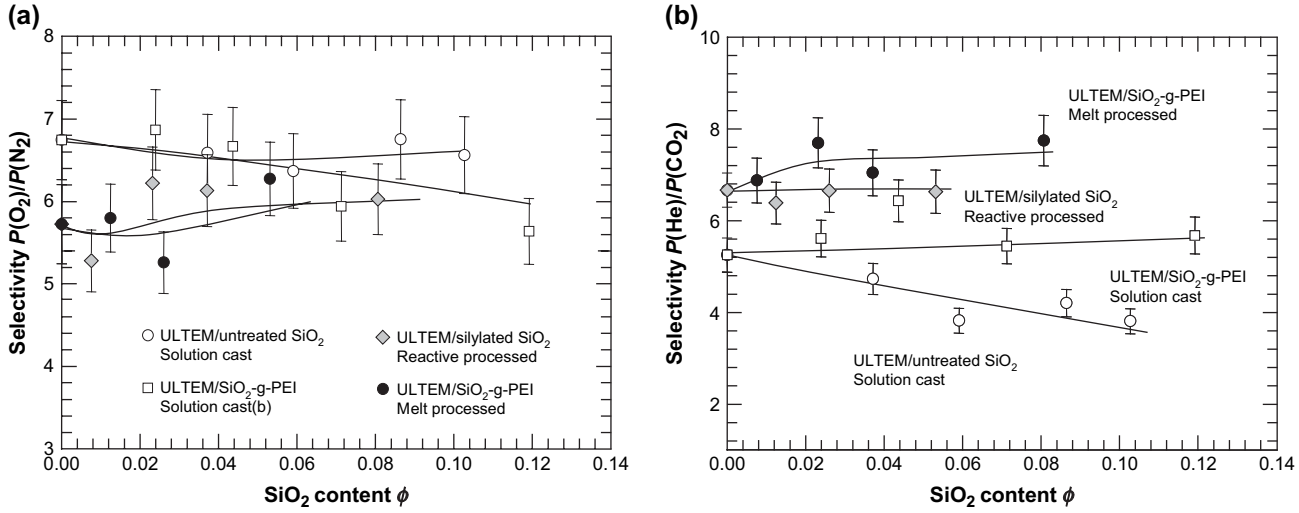

Fig. 15. Selectivity in ULTEM®/SiO_2 nanocomposite membranes made by solution casting and melt processing as a function of SiO_2 weight fraction: (a) O_2/N_2 selectivity and (b) He/CO_2 selectivity.

Acknowledgment

This work was supported by the National Science Foundation (Grant number DMR-0238979) and the Separation Research Program at the University of Texas at Austin. The authors wish to thank Professor W.J. Koros for helpful discussions relating to techniques for implementing the silane coupling agent strategy.

References

[1] Sinha Ray S, Okamoto M. Polymer/layered silicate nanocomposites: a review from preparation to processing. Prog Polym Sci 2003;28:1539–641.
[2] Giannelis EP. Polymer-layered silicate nanocomposites: synthesis, properties and applications. Appl Organomet Chem 1998;12:675–80.
[3] Giannelis EP. Polymer layered silicate nanocomposites. Adv Mater 1996;8:29–35.
[4] Yano K, Usuki A, Okada A. Synthesis and properties of polyimide-clay hybrid films. J Polym Sci Part A Polym Chem 1997;35:2289–94.
[5] Dennis HR, Hunter DL, Chang D, Kim S, Ehite JL, Cho JW, et al. Effect of melt processing condition on the extent of exfoliation in organoclay-based nanocomposites. Polymer 2001;42:9513–22.
[6] Fornes TD, Paul DR. Structure and properties of nanocomposites based on nylon-11 and -12 compared with those based on nylon-6. Macromolecules 2004;37:7698–709.
[7] Hotta S, Paul DR. Nanocomposites formed from linear low density polyethylene and organoclays. Polymer 2004;45:7639–54.
[8] Takahashi S, Goldberg HA, Feeney CA, Karim DP, Farrell M, O'Leary K, et al. Gas barrier properties of butyl rubber/vermiculite nanocomposite coatings. Polymer 2006;47:3083–93.
[9] Takahashi S, Paul DR. Gas permeation in poly(ether imide) nanocomposite membranes based on surface treated silica. Part 1: no chemical coupling to matrix. Polymer, pending editor's decision (POLYMER-06-1460).
[10] Mahajan R, Zimmerman CM, Koros WJ. Fundamental and practical aspects of mixed matrix gas separation membranes. ACS Symp Ser 1999;733:277–86.
[11] Mahajan R, Koros WJ. Mixed matrix membrane materials with glassy polymers. Part 1. Polym Eng Sci 2002;42:1420–31.
[12] Zimmerman CM, Singh A, Koros WJ. Tailoring mixed matrix composite membranes for gas separations. J Membr Sci 1997;137:145–54.
[13] Vu DQ, Koros WJ, Miller SJ. Mixed matrix membranes using carbon molecular sieves I. Preparation and experimental results. J Membr Sci 2003;211:311–34.
[14] Vu DQ, Koros WJ, Miller SJ. Mixed matrix membranes using carbon molecular sieves II. Modeling permeation behavior. J Membr Sci 2003;211:335–48.
[15] Moore TT, Mahajan R, Vu DQ, Koros WJ. Hybrid membrane materials comprising organic polymers with rigid dispersed phases. AIChE J 2004;50:311–21.
[16] Merkel TC, Freeman BD, Spontak RJ, He Z, Pinnau I, Meakin P, et al. Sorption, transport, and structural evidence for enhanced free volume in poly(4-methyl-2-pentyne)/fumed silica nanocomposite membranes. Chem Mater 2003;15:109–23.
[17] Merkel TC, Freeman BD, Spontak RJ, He Z, Pinnau I, Meakin P, et al. Science 2002;296:519–22.
[18] Merkel TC, He Z, Pinnau I, Freeman BD, Meakin P, Hill AJ. Sorption and transport in containing nanoscale fumed silica. Macromolecules 2003;36:8406–14.
[19] Zhong J, Lin G, Wen W, Jones AA, Kelman S, Freeman BD. Translation and rotation of penetrants in ultrapermeable nanocomposite membrane of poly(2,2-bis(trifluoromethyl)-4,5-difluoro-1,3-dioxole-co-tetrafluoroethylene) and fumed silica. Macromolecules 2005;38:3754–64.
[20] He Z, Pinnau I, Morisato A. Novel nanostructured polymer-inorganic hybrid membranes for vapor-gas separation. ACS Symp Ser 2004;876:218–33.
[21] Winberg P, DeSitter K, Dotremont C, Mullens S, Vankelecom IFJ, Maurer FHJ. Free volume and interstitial mesopores in silica filled poly(1-trimethylsilyl-1-propyne) nanocomposites. Macromolecules 2005;38:3773–82.
[22] Laura DM, Keskkula H, Barlow JW, Paul DR. Effect of glass fiber surface chemistry on the mechanical properties of glass fiber reinforced, rubber-toughened nylon 6. Polymer 2002;43:4673–87.
[23] Vankelecom IFJ, Van den broeck S, Merckx E, Geerts H, Grobet P, Uytterhoeven JB. Silylation to improve incorporation of zeolites in polyimide films. J Phys Chem 1996;100:3753–8.
[24] Linde HG. Adhesive interface interactions between primary aliphatic amine surface conditioners and polyamic acid/polyimide resins. J Polym Sci Part A Polym Chem 1982;20:1031–41.
[25] Buchwalter LP, Oh TS, Kim J. Adhesion of polyimides to ceramics: effects of aminopropyltriethoxysilane and temperature and humidity exposure on adhesion. J Adhes Sci Technol 1991;5(4):333–43.
[26] Fukano K, Kageyama E. Study of radiation-induced polymerization of vinyl monomers adsorbed on inorganic substances. VII. Effect of

pretreatment temperature of silica gel on styrene–silica gel system. J Polym Sci Polym Chem Ed 1976;14:1743–51.
[27] O'Brien KC, Koros WJ, Barbari TA, Sanders ES. A new technique for the measurement of multicomponent gas transport through polymeric films. J Membr Sci 1986;29:229–38.
[28] Barbari TA, Koros WJ, Paul DR. Gas transport in polymers based on bisphenol A. J Polym Sci Part B Polym Phys 1988;26:709–27.
[29] Koros WJ. Ph.D. dissertation. The University of Texas at Austin; 1977.
[30] Dymond JH, Smith EB. The virial coefficients of pure gases and mixtures: a critical compilation. New York: Oxford University Press; 1980.
[31] Maxwell JC. A treatise on electricity and magnetism, vol. 1. London: Oxford University Press; 1873.
[32] Barrer RM, Barrie JA, Raman NK. Solution and diffusion in silicone rubber II. The influence of fillers. Polymer 1962;3:605–14.
[33] Barrer RM, Barrie JA, Rogers MG. Heterogeneous membranes: diffusion in filled rubber. J Polym Sci Part A Polym Chem 1963;1:2565–86.
[34] Koros WJ, Chan AH, Paul DR. Sorption and transport of various gases in polycarbonate. J Membr Sci 1977;2:165–90.
[35] Paul DR, Yampol'skii YP, editors. Polymeric gas separation membranes. Boca Raton: CRC press; 1994.